

# A Comparison of ESAC and FK Methods of Estimating Phase Velocity Using Arbitrarily Shaped Microtremor Arrays

by Michihiro Ohori, Arihide Nobata, and Kunio Wakamatsu

**Abstract** Focusing on a comparison of the accuracy of the extended spatial autocorrelation (ESAC) method and the frequency–wavenumber spectrum (FK) method, we carried out short-period microtremor measurements of arbitrarily shaped array configurations at a site with a well-known velocity structure at shallow depths. Using both techniques, we measured phase velocities for frequencies between 2.5 Hz and 13.5 Hz and compared the results with the theoretical Rayleigh-wave-dispersion characteristics of both the fundamental and the first higher modes calculated from the *PS* logging data. Next, we tried to estimate the *S*-wave velocity structure to a depth of 43 m by fitting the theoretically calculated phase velocities to the experimental data, taking into consideration both the higher mode contributions as well as the fundamental mode. The theoretical dispersion characteristics were successfully fitted to the results analyzed by the ESAC method but not by the FK method. The estimated *S*-wave velocity structure from the ESAC method results was in good agreement with the *PS* logging profile. We also confirmed, using the model, that the *S*-wave transfer function due to vertical incidence coincided with that from the *PS* logging data. As a result of the study, we conclude that the ESAC method gives more accurate results than the FK method in determining the Rayleigh-wave phase velocity from records of short-period microtremors using arbitrarily shaped array configurations. The ESAC method can also provide a better estimate of the *S*-wave velocity structure and site amplification than the FK method.

## Introduction

It is widely recognized that the determination of *S*-wave velocity structure is important in accurately predicting strong ground motion. Such information is required for aseismic design and in evaluating the damage distribution caused by earthquakes (e.g., Horike, 1996; Kawase, 1996; Kawase *et al.*, 1998). Since the pioneering work of Horike (1985) and Okada (1986), microtremor-array measurement has been recognized as one of the attractive and convenient exploration methods for determining the *S*-wave velocity, especially in highly populated urban areas where much consideration must be given to the vibrational environment.

The frequency–wavenumber spectrum (FK) method and the spatial autocorrelation (SAC) method are two data-processing techniques used to obtain phase velocities from microtremor-array measurements. The FK method is also separated into two subtypes: the maximum-likelihood method (high-resolution method) proposed by Capon (1969) and the beamforming method (conventional method) proposed by Lacoss *et al.* (1969). The FK method has been widely used in earlier studies by various researchers, for example, Asten and Henstridge (1984), Horike (1985, 1996), Okada (1986, 1994), Okada *et al.* (1987), Matsushima and

Okada (1989, 1990), Sato *et al.* (1991), Tokimatsu *et al.* (1991, 1992a, 1992b), Yamanaka *et al.* (1994), Miyakoshi *et al.* (1994, 1998), Kagawa (1996), Ishida *et al.* (1998), Milana *et al.* (1996), Suetomi and Nakamura (1996), Kagawa *et al.* (1998), Kataoka and Kawase (1998), Kawase *et al.* (1998), Liu *et al.* (2000), Satoh *et al.* (2001), and Kudo *et al.* (2002).

The SAC method, originally proposed by Aki (1957, 1964), has the potential to provide more accurate results than the FK method. However, it has been used by only a few researchers, namely, Okada (1986), Okada *et al.* (1987), Tokimatsu *et al.* (1992a), Okada (1994), Matsuoka *et al.* (1996), Miyakoshi and Okada (1996), and Chouet *et al.* (1998). This limited use may arise from the disadvantage that in the SAC method, the array configuration must be circular. Especially in urban areas, such an array configuration is difficult to achieve and sometimes sensors must be deployed along streets, and L-shaped, T-shaped, or cross-shaped arrays must be used, for example, by Asten and Henstridge (1984), Horike (1985), Sato *et al.* (1991), and Milana *et al.* (1996). In such cases, the FK method has been considered the only choice for data processing. To remedy this

disadvantage of the SAC method, that is, the circular-array configuration, Ling and Okada (1993) and Okada (1994) proposed the extended spatial autocorrelation (ESAC) method, which makes it possible to design arbitrarily shaped arrays. Using microtremor records of semicircular arrays and a slightly transformed circular configuration, they confirmed that the ESAC method provides results for phase velocity that are as accurate as those using the FK method. However, the ESAC method has not been used to analyze arbitrarily shaped arrays. In addition, the applicability of the ESAC method as well as of the SAC method to short-period microtremor records remains unknown.

In this article, we report array measurements of microtremors made using arbitrarily-shaped configurations at a site with well-known underground structure. The phase-velocity data was analyzed using both the ESAC method and the FK method. From the small-aperture-array measurements conducted, phase-velocity values were determined for frequencies ranging from 2.5 Hz to 13.5 Hz. The phase-velocity dispersions obtained using both methods were compared with those calculated from the *PS* logging data. The *S*-wave velocity structures were also estimated on the basis of the experimental dispersion characteristics. Finally, transfer functions calculated from the estimated structure in the present study were compared with those based on the *PS* logging data.

### Short Description of Analytical Procedure

To obtain the phase velocity from data sets of a microtremor-array measurement, we used the maximum-likelihood method of Capon (1969) as the FK method and the ESAC method proposed by Ling and Okada (1993) and Okada (1994). The FK method is well known and can be found in many articles, for example, Capon (1969), Okada (1986), and Tokimatsu *et al.* (1992b). On the other hand, the ESAC method proposed by Ling and Okada (1993) and Okada (1994) may not be well known, because these articles were written in Japanese and may not be well circulated. Therefore, we present a short description of the analytical procedure used in the ESAC method, which was developed from the SAC method by Aki (1957, 1964).

Using a Fourier transform of the array data, normalized cross spectra between the *l*th and *n*th seismometers are obtained as below:

$$S_{ln}(f) = \frac{\frac{1}{M} \sum_{m=1}^M m S_{ln}(f)}{\sqrt{\frac{1}{M^2} \sum_{m=1}^M m S_{ll}(f) \sum_{m=1}^M m S_{mm}(f)}}, \quad (1)$$

where *f* is the frequency (in Hz),  $m S_{ln}(f)$  is the cross spectrum for the *m*th segment, and *M* is the total number of segments. This procedure is based on the direct segment method (Capon, 1969).

Let us consider an array design using *N* seismometers for the SAC method. It is assumed that the center-element seismometer is located at the origin, and the others are distributed on a circle with radius *r* with an equally spaced azimuth. The normalized cross spectra  $S_{ln}(f)$  obtained from equation (1) are hereafter renamed  $S_{ln}(f, r_{ln})$ , where  $r_{ln} = \{(x_n - x_l)^2 + (y_n - y_l)^2\}^{1/2}$ . Considering that *n* = 0 corresponds to the origin and  $r_{0n} = r$ , the azimuthally averaged spatial autocorrelation function is defined as

$$S(f, r) = \frac{1}{N-1} \sum_{n=1}^{N-1} \text{Reall} |S_{0n}(f, r)|. \quad (2)$$

The apparent phase velocity *c*(*f*) satisfies the following equation

$$S(f, r) = J_0\left(\frac{2\pi f r}{c(f)}\right), \quad (3)$$

where  $J_0$  is the zero-order Bessel function. A detailed derivation of this relationship can be found in Aki (1957, 1964), and Okada (1994). By fitting the azimuthally averaged spatial autocorrelation function to the Bessel function, the phase velocity *c*(*f*) can be obtained. In determining *c*(*f*) from equation (3) using the SAC method, we must select one of the following conditions to obtain the solution; either *r* is constant (condition 1) or *f* is constant (condition 2). It is noted that condition 2 leads to better results than condition 1 because *c*(*f*) is a function of frequency (Ling and Okada, 1993; Okada, 1994).

The ESAC method is derived from the SAC method by using condition 2 to remedy the constraint in the array design, and *c*(*f*) is found to satisfy the following equation in the least-squares sense, instead of equation (3):

$$S_{0n}(f, r_{0n}) = J_0\left(\frac{2\pi f r_{0n}}{c(f)}\right) (n = 1, 2, 3, \dots, N-1). \quad (4)$$

The following equation is used to determine the error in evaluating *c*(*f*). Because there is only one unknown in this equation, it is easy to obtain a solution. In this article, the least-squares algorithm proposed by Marquardt (1963) is used to obtain the results:

$$\text{Error} = \sum_{n=1}^{N-1} \left[ S_{0n}(f, r_{0n}) - J_0\left(\frac{2\pi f r_{0n}}{c(f)}\right) \right]^2. \quad (5)$$

### Microtremor-Array Measurement and Data Processing

#### Test Field and Geological Information

The test field for this study was the grounds of the authors' research institute located in Kiyose, Tokyo, Japan. At this site, mainly for the purpose of building construction, a number of standard penetration tests up to 16 m deep had

been carried out to cover the complete test field. The near-surface underground structure is mainly horizontally stratified layers. This flat surface is covered to a depth of 0.3–0.8 m with surface soil or reclaimed soil. Beneath that, Kanto Loam and Musashino Gravel are layered over the Upper Tokyo Formation, with thicknesses of 4–6 m and 4–6 m, respectively. In addition, *PS* logging had been carried out at this site down to 49 m, so that the shallow-velocity structure was known to be as shown in Table 1.

#### Array Configuration

Figure 1 shows two array configurations of different sizes that we used. These configurations were named S1 and S2. For the S1 array, 14 sensors were placed at 5-m intervals. The maximum array length in the *X* direction was 20 m and in the *Y* direction was 45 m. For the S2 array, 13 sensors were spaced approximately 20 m apart. The maximum array length in the *X* direction was 120 m and that in the *Y* direction was 120 m. The arrays were in the shape of the letter L. These arrays are not ideal configurations because we had strict constraints in deploying the sensors; inside the property were many laboratory buildings, experimental facilities, and some new buildings under construction. However, we consider that similar conditions will exist when array measurements are made in urban areas. It may be considered that this study is a realistic test to ascertain the applicability of the ESAC and the FK methods in such areas.

The minimum wavelength detected in the measurements is twice the shortest distance between sensors deployed in the array; this is determined by the Nyquist wavenumber. On the other hand, the maximum wavelength seems to vary case by case because it is determined empirically. It has been recognized that the maximum wavelength detected in array observations varies from twice to several times the largest sensor spacing, as in previous studies, such as those of Horike (1985), Okada (1994), and Satoh *et al.* (2001). In this study, for safety we decided to use twice the largest sensor spacing as the maximum wavelength. Therefore, we estimate the detectable wavelengths from the S1 array as 10–40 m and from the S2 array as 40–240 m.

#### Measurement

Measurements were carried out during the day on 1 March 1997. We used vertical-component velocity sensors, which were each connected to the amplifier by an extension cable. The system provided records proportional to the velocity of the ground motion in the frequency range 0.5–30 Hz. Signals detected by the sensors were amplified and recorded on magnet-optical disks after digitalization inside a recorder. The sampling frequency and recording time were respectively set to 200 Hz and 15 min for the S1 array and 100 Hz and 30 min for the S2 array.

#### Data Processing

For analytical convenience, the data were divided into several sets, comprising six data sets containing 150 sec for

Table 1  
Underground Structure of the Test Field Obtained from *PS* Logging

Layer No.	Thickness (m)	Density (ton/m <sup>3</sup> )	$V_p$ (m/sec)	$V_s$ (m/sec)
1	5.65	1.40	230.0	130.0
2	6.35	2.00	620.0	380.0
3	6.00	2.00	880.0	460.0
4	8.70	2.00	1770.0	460.0
5	8.90	2.00	1770.0	430.0
6	7.40	2.10	1920.0	520.0
7	∞	2.10	1920.0	600.0

the S1 array and eight data sets containing 300 sec for the S2. Each data set included 30,000 data points. In calculating the cross spectra, each data set was divided again into 6 or 12 segments of 25 sec and transformed into the frequency domain with the fast Fourier transform. The cross spectrum for each segment was obtained and smoothed by a Parzen window with a width of 0.2 Hz. Then the normalized cross spectrum for each data set was calculated using equation (1) and used for analysis. To use the fast Fourier transform, null data were added to each segment to make the total data points up to 4,096 or 8,192. Other conditions were tested, but no significant differences were found in the obtained phase velocities. Our records included some noise from different sources, such as traffic noise from surrounding roads, a repavement construction along the eastern side road, factory noise, and so on. However, we used all of the data for the phase-velocity calculation, because in the case of short-period microtremors, it is difficult to recognize by sight which part of the waveform is good or bad. The phase-velocity results for each data set using the ESAC and FK methods were selected using the following criteria: (1) the corresponding wavelength must be between twice the minimum sensor spacing and twice the maximum sensor spacing, (2) the phase velocity for a particular frequency must not be twice as large as that for adjacent frequencies in each data set, and (3) the number of effective phase-velocity results for each frequency must not be less than half the number of data sets.

#### Phase-Velocity Results

In Figure 2, we compare the phase-velocity results obtained using the ESAC method with theoretical ones. The averaged phase velocity using the ESAC method is indicated with solid rectangles. The standard deviation from the average phase velocity is indicated with an error bar from each solid rectangle. The theoretical phase velocity of the Rayleigh wave is expressed with two solid lines for the fundamental and the first higher modes. These were calculated from the underground structure in Table 1. Figure 2 shows that most of the results from the ESAC method are in good agreement with the theoretical results of the fundamental

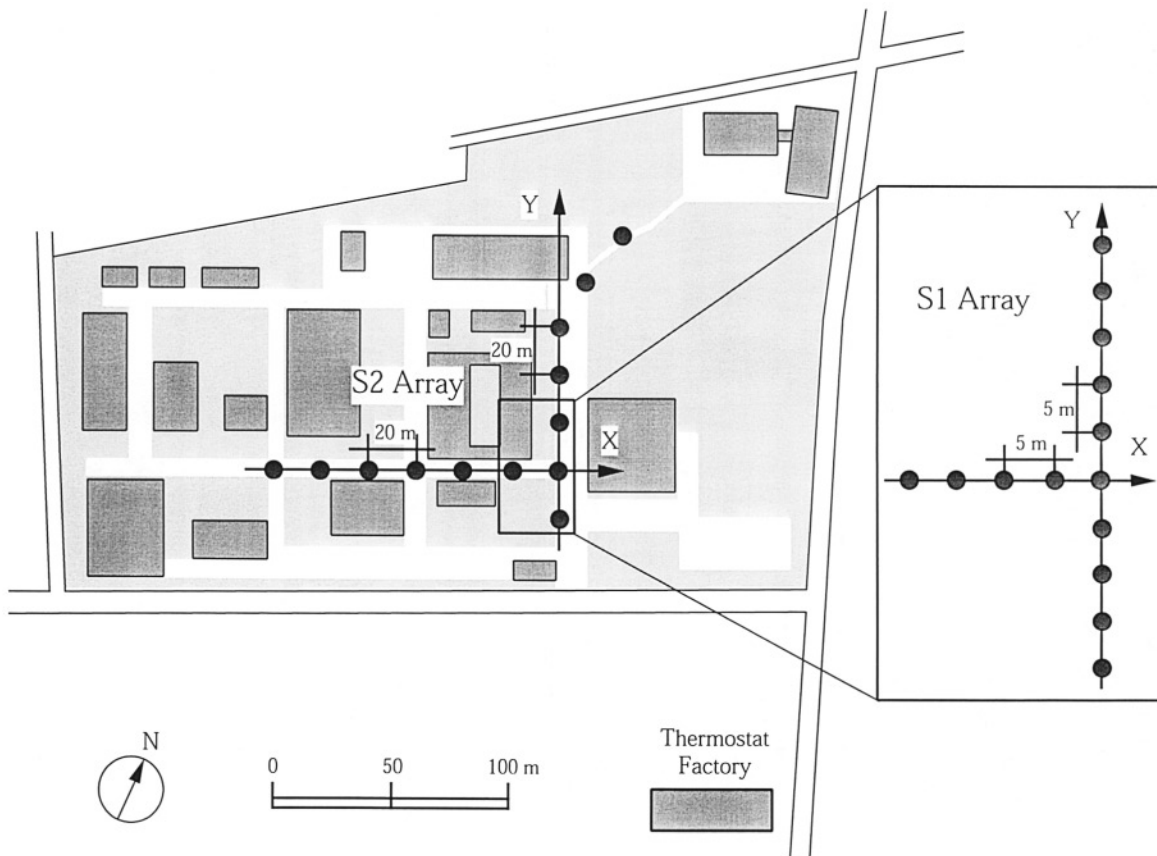


Figure 1. Array configurations conducted in microtremor measurements. The test field is located in Kiyose, Tokyo, Japan ( $35.7861^{\circ}$  N,  $139.5397^{\circ}$  E). The S1 array comprises 14 vertical-component sensors spaced at 5-m intervals and the S2 array of 13 sensors spaced at 20-m intervals.

mode, except between 6.5 Hz and 8.5 Hz, wherein the estimated results correspond to the first higher mode. In addition, near 5.5 Hz, the measured phase velocities scatter between the two modes of the theoretical Rayleigh wave.

In Figure 3, we show examples of fitting the Bessel function to the experimental data of the SAC function. The horizontal axis denotes the distance between the central element and the other sensor locations. In this figure, a solid circle indicates observed data. The solid line indicates results using the estimated velocity. Two other broken lines used the estimated velocity with +10% and -10% variance. It can be seen that the estimated values agree well with the experimental data.

In Figure 4, we compare the obtained phase velocity using the FK method with theoretical ones. From this figure, we observe that phase-velocity results from the FK method seem to correspond to the fundamental mode for frequencies below 5 Hz and scatter between the two modes for frequencies  $>10$  Hz. For the remaining frequencies, however, the experimental results are closer to the first higher mode than the fundamental mode. In addition, the results from the FK method are fewer in the frequency range between 5.5 Hz and 8.5 Hz in comparison with those from the ESAC method.

In this frequency range, the FK spectrum tended to resolve unclear peaks. Thus, most of the phase-velocity results became unstable, that is, too high or too low. Consequently, such estimated results were rejected mainly by the array's detectable-wavelength criterion and partially by the remaining criteria.

Examples of the FK spectra for a data set are shown in Figure 5. Contours of the log-normalized FK spectrum  $[-10\log(P(f,k)/P(f,k_{peak}))]$  for each frequency are drawn in steps of 1 dB. A circle and a straight line denote the corresponding peak velocity and azimuth, respectively, for the wavenumber vector at the peak spectrum amplitude. These examples correspond to results coming from the northeastern road crossing and a southeastern thermostat factory, respectively. In other cases, the arrival direction coincided with a southeastern crossing. For frequencies less than 10 Hz, most of the arrival directions determined by the FK spectrum peak clustered into these three azimuths. These peak directions may imply that waves propagating to the array were excited by traffic loads near two road crossings and by a factory's activity, respectively (see Fig. 1). On the other hand, for frequencies  $>10$  Hz, the FK spectrum resolved several peaks with various azimuths, implying the presence of multiple

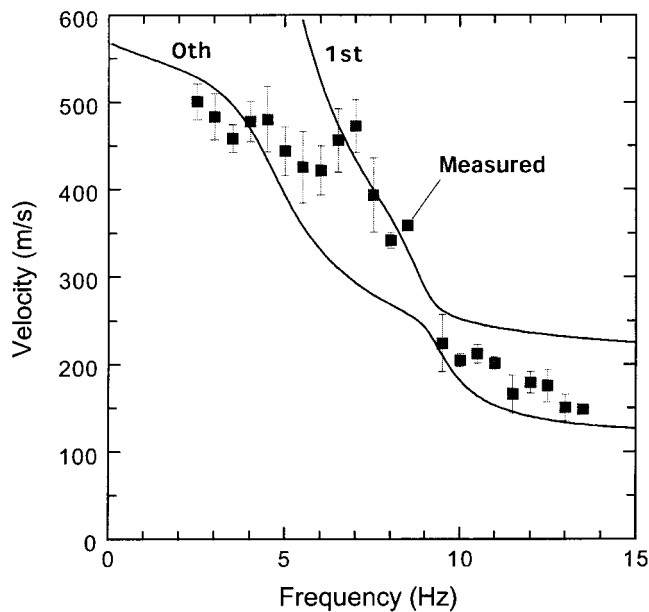


Figure 2. Phase-velocity results obtained from the ESAC method for each array. Average velocities for particular frequencies are plotted with solid rectangles. The standard deviations are plotted with solid bars. The theoretical phase velocity of the Rayleigh wave calculated from the *PS* logging model in Table 1 is expressed with two solid lines for the fundamental and the first higher modes.

sources. In such cases, we investigated the phase velocities determined from the first peak to the third peak and found that most of the experimental phase velocities were scattered between the fundamental mode and the first higher mode of the theoretical Rayleigh wave calculated from the *PS* logging model in Table 1. Simulation results by Okada (1994) and Liu *et al.* (2000) pointed out that the FK method can detect the phase velocity accurately in cases of multiple sources. In addition, in most previous studies using the FK method, the first peak of the FK spectrum automatically determined the phase velocity. Therefore, we use only the first peak in the FK method to compare the consistency of the FK method and the ESAC method simply and automatically.

### Estimation of the *S*-Wave-Velocity Structure and Transfer Function

#### Apparent Phase Velocity of Rayleigh Wave Including the Higher-Mode Contribution

In estimating the *S*-wave-velocity structure from the phase-velocity data, most previous studies were carried out on the assumption that the detected waves were mainly composed of the fundamental mode of the Rayleigh wave. However, as shown in Figures 2 and 4, the present study from the microtremor-array records seems to detect the first higher mode of the Rayleigh wave in the frequency range from about 6 Hz to 9 Hz. If this is so, then to estimate the *S*-wave-

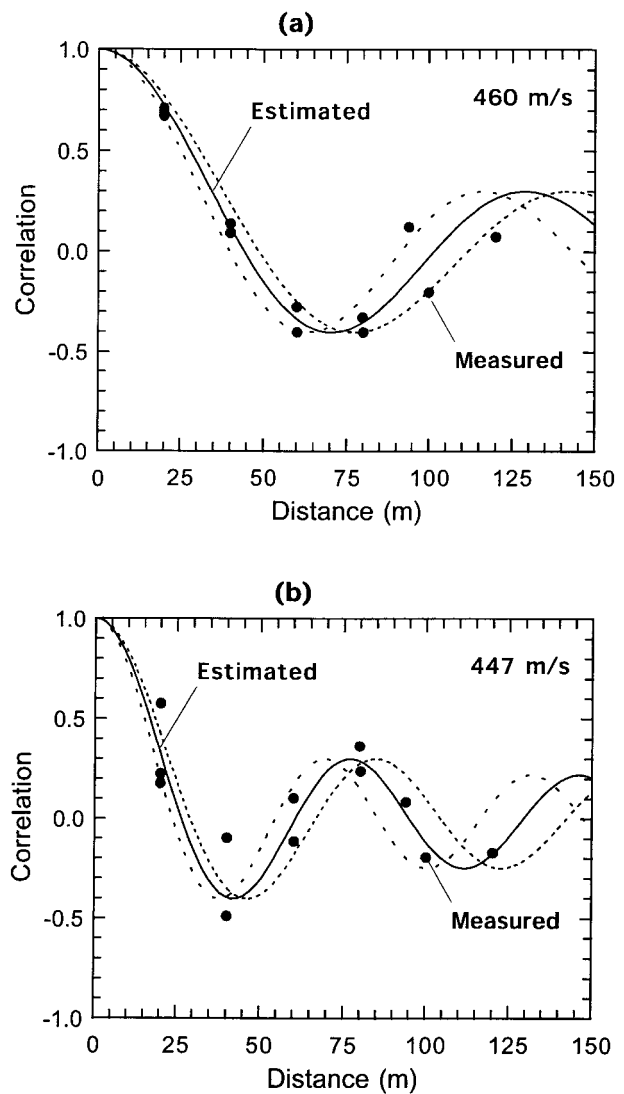


Figure 3. Example of SAC functions for the S2 array from the ESAC method. The observed data between the central element and other seismometers are plotted with solid circles, and the estimated ones with solid lines. The two broken lines are drawn for calculations made with a 10% variance in the estimated velocity. The estimated phase velocity is written in the upper right-hand corner. (a) 4.0 Hz; (b) 6.0 Hz.

velocity structure from the detected phase velocity data we need to consider the contribution of the higher modes of the Rayleigh wave to the apparent phase velocity. For short-period microtremor measurements, this phenomenon has been observed in previous studies, such as Tokimatsu *et al.* (1991, 1992a, 1992b). In addition, Tokimatsu *et al.* (1992c) also formulated the apparent phase velocity determined from microtremor-array data as a superimposition of the multiple-mode Rayleigh wave. Assuming that both the sources and receivers are located only on the surface, Tokimatsu *et al.* (1992c) proposed that the apparent phase velocity,  $c_{si}(f)$ , from array records, should be related to the multiple-mode Rayleigh waves as

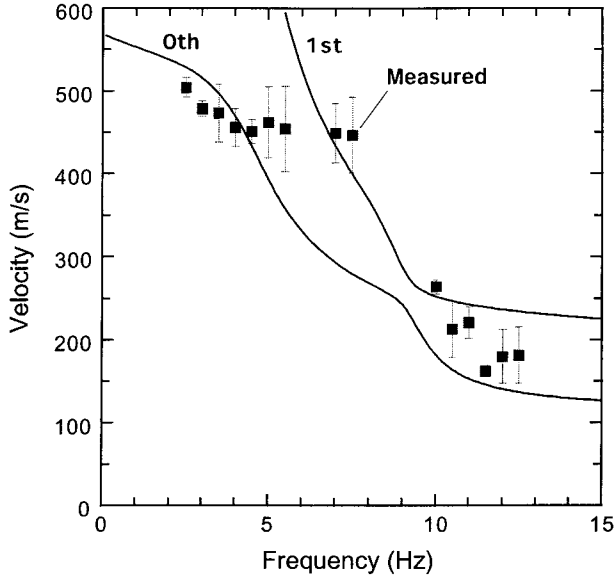


Figure 4. Phase-velocity results obtained from the FK method for each array. Other conditions are the same as those in Figure 2.

$$\cos\left(\frac{2\pi fr}{c_{si}(f)}\right) \sum_{m=0}^M A_m^2(f) c_m(f) = \sum_{m=0}^M A_m^2(f) c_m(f) \cos\left(\frac{2\pi fr}{c_m(f)}\right), \quad (6)$$

where  $c_m(f)$  and  $A_m(f)$  denote the phase velocity of the  $m$ -th mode Rayleigh wave and the corresponding medium response (Harkrider, 1964), respectively. In the equation (6),  $M$  is the maximum order of mode for each frequency, and  $r$  is the shortest distance between sensors. Verification of the aforementioned equation was done using records from microtremor-array measurements (see Tokimatsu *et al.*, 1992b).

Using equation (6), we can calculate the apparent phase velocity of the Rayleigh wave for the underground structure in Table 1. In Figure 6a, the apparent phase velocity proposed by Tokimatsu *et al.* (1992c) is shown with a solid circle, and the phase velocities of the fundamental mode and the higher modes are shown with solid or dotted lines. In Figure 6b, we also show the medium response  $A_m(f)$ , normalized by the corresponding wavenumber  $\sqrt{2\pi f/c_m(f)}$ . Note that the calculated apparent phase velocity coincides with that of the first higher mode between 6 Hz and 9 Hz, in which the medium response for the first higher mode dominates that for the fundamental mode. In the other frequency range, the apparent phase velocity is consistent with the fundamental mode. The second and third higher modes do not make a significant contribution to the apparent phase velocity, because the response of the medium for those modes is relatively small. We can observe that the apparent phase velocity dispersion in Figure 6a is in good agreement with the observed data shown in Figures 2 and 4. In the following section, we use equation (6) to invert the  $S$ -wave-velocity structure from the experimental phase-velocity data.

### Estimation of $S$ -Wave-Velocity Structure

We attempted to estimate the  $S$ -wave velocity using the experimental phase-velocity results from the ESAC method and the FK method. Considering the sensitivity to the Rayleigh wave dispersion and geological information mentioned previously, we determined only the  $S$ -wave-velocity structure. Other parameters such as the  $P$ -wave velocity, density, and thickness of each layer are set to the values in Table 1. After obtaining the initial model by trial and error, we determined the  $S$ -wave-velocity model using the simplex downhill method (Nelder and Mead, 1965) to minimize the discrepancy between the theoretical values and the experimental data evaluated by the following equation:

$$Error = \sum_{l=1}^{NF} (c_{si}(f_l) - c_{obs}(f_l))^2 / \sum_{l=1}^{NF} c_{obs}(f_l)^2, \quad (7)$$

where  $c_{obs}(f)$  and  $c_{si}(f)$  denote the experimental phase-velocity data at frequency  $f_l$  and the theoretical one, which is derived from equation (6). The total of frequencies,  $NF$ , is 21 for the ESAC method and 15 for the FK method. In inversion, the  $S$ -wave velocity of the deepest layer was fixed to 600 m/sec, derived from the  $PS$  logging data. This value was chosen because it is almost the same as the estimated  $S$ -wave velocity obtained from the other exploration results for the uppermost Pleistocene layer of thickness 500 m, for example, seismic-refraction experiments, 580 to 630 m/sec, by Shima *et al.* (1978). Therefore, we estimated the  $S$ -wave velocity for six layers above the bottom layer. The experimental data for the ESAC method were successfully matched as shown in Figure 7, but not so for the data obtained using the FK method. As mentioned before, the phase-velocity results from the FK method are fewer for frequencies between 5.5 Hz and 8.5 Hz and failed to constrain the theoretical one. In Figure 7, we observe that the experimental dispersion characteristics from the ESAC method are well reproduced by the estimated model. The good agreement between the phase-velocity dispersion of the estimated model and the  $PS$  logging model suggests that the apparent phase velocity in the frequency range from 6 Hz to 9 Hz has a strong contribution from the first higher mode Rayleigh wave. In Table 2, we show the estimated  $S$ -wave-velocity model using the ESAC method compared with the  $PS$  logging data. The discrepancy between the estimated  $S$ -wave velocity and the  $PS$  logging data is within 12%.

Figure 8 shows the transfer functions for  $S$ -wave vertical incidence using the estimated model based on the phase-velocity results from the ESAC method and the  $PS$  logging data, featured in Table 2. The damping factor of each layer is assumed to be 1%. We observe good agreement between the two transfer functions, suggesting that the ESAC method is a very useful technique for evaluation of site amplification.

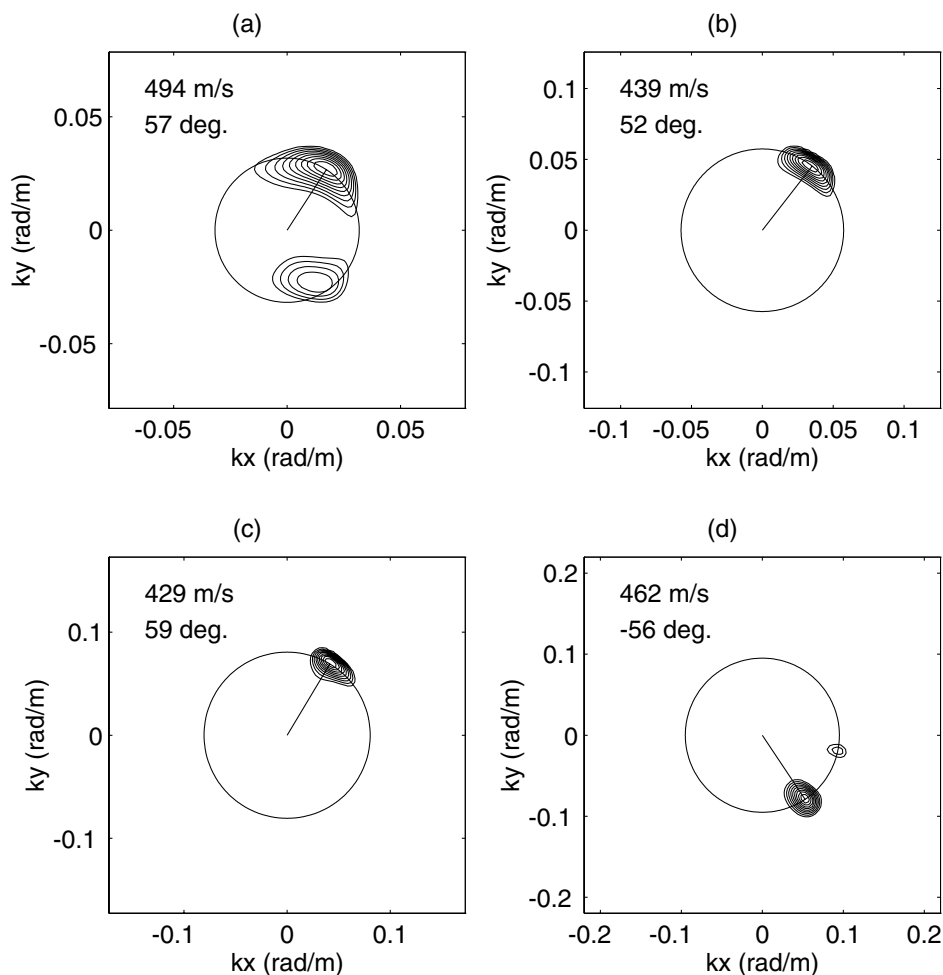


Figure 5. Example of contour maps showing the FK spectra for the S2 array. The phase velocity and arrival direction determined from the maximum peak are written in the upper left-hand corner, indicated as a circle and a straight line from the origin. The arrival direction is measured counterclockwise from the east. (a) 2.5 Hz; (b) 4.0 Hz; (c) 5.5 Hz; (d) 7.0 Hz.

### Conclusions

The FK method has been used by many researchers as a tool to analyze data from array measurements of microtremors. We believe the ESAC method, which is an alternative technique, has the potential to produce more accurate and stable results than the FK method. To test this, verification should be done for various soil conditions and by various researchers. Focusing on a direct comparison of results obtained using the FK method and the ESAC method, we carried out short-period microtremor measurements with arbitrarily shaped array configurations at a site with a well-known velocity structure.

First, we obtained the phase velocity for frequencies between 2.5 Hz and 13.5 Hz using the two techniques and compared them with the theoretical Rayleigh-wave dispersions based on the *PS* logging data. We found that the phase-velocity results from the ESAC method, in frequency ranges

below about 5 Hz and above 10 Hz, corresponded to the Rayleigh-wave fundamental mode, whereas in the range from 6 Hz to 9 Hz, they corresponded to the first higher mode. Similar phase-velocity results were obtained from the FK method. However, the FK method gives fewer results between 5.5 Hz and 8.5 Hz compared with the ESAC method. In this frequency range, the FK spectrum tended to resolve unclear peaks. Thus, most of the phase-velocity results became unstable, that is, too high or too low. Consequently, such estimated results were rejected mainly by the array's detectable-wavelength criterion and partially by the remaining criteria.

Next, using the experimental phase-velocity dispersion characteristics, we endeavored to estimate the *S*-wave-velocity structure at a depth of 43 m. In inversion, both the Rayleigh-wave fundamental mode and higher modes were considered. For the ESAC method, fitting the apparent phase

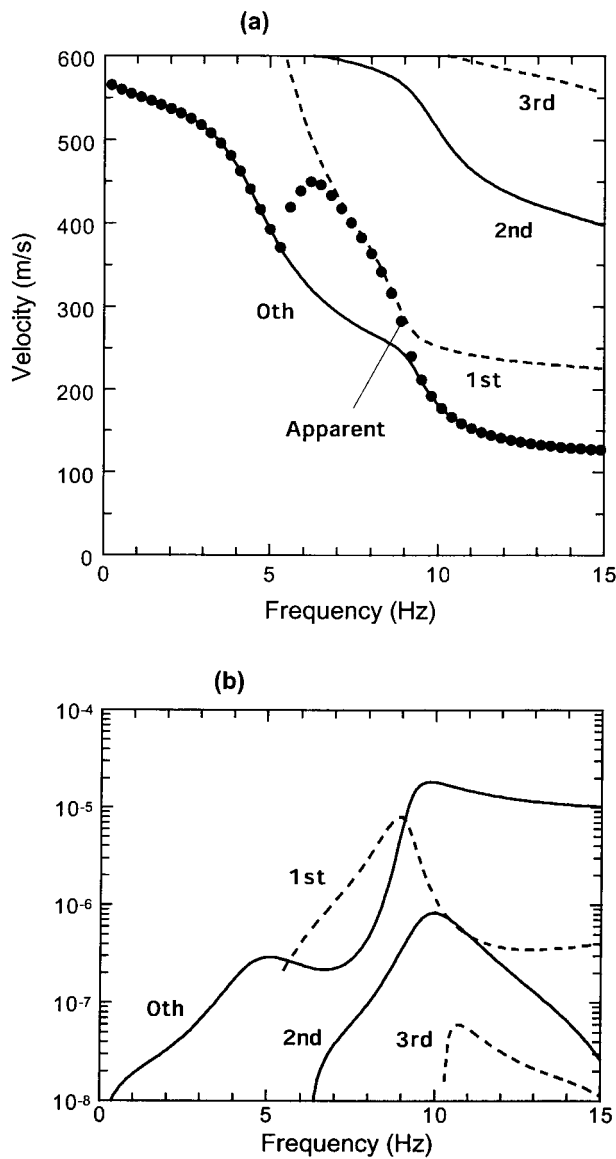


Figure 6. Apparent phase-velocity dispersions of the theoretical Rayleigh wave and the medium response function from the *PS* logging model in Table 1. (a) Apparent phase velocity proposed by Tokimatsu *et al.* (1992c) is shown with a solid circle, and the phase velocities of the fundamental mode and the higher modes are shown with solid or dotted lines. (b) The medium response function  $A_m(f)$  normalized by the corresponding wavenumber  $\sqrt{2\pi f/c_m(f)}$  is indicated.

velocity of the theoretical Rayleigh wave to the experimental data was carried out successfully, and the *S*-wave-velocity structure was obtained. On the other hand, we were unable to fit them to the data from the FK method.

Finally, the transfer function for the estimated *S*-wave-velocity structure found by using the ESAC method results was compared with that from the *PS* logging data. Excellent agreement between these two transfer functions was observed.

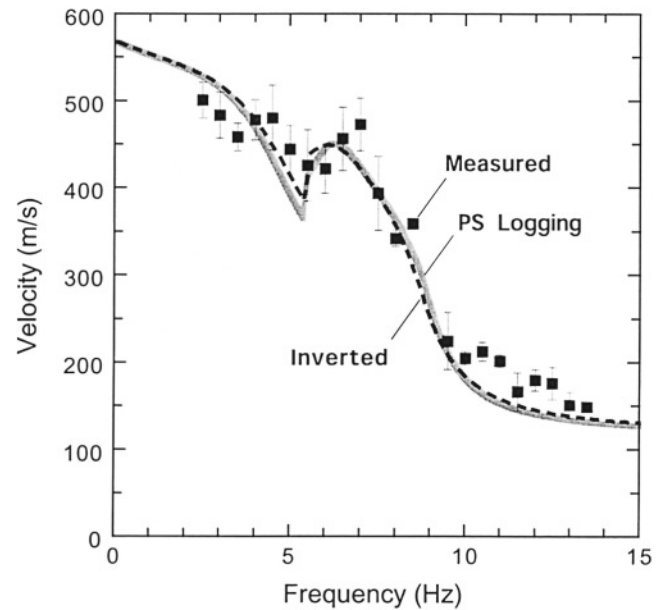


Figure 7. Apparent phase-velocity dispersions of the Rayleigh wave from the *PS* logging model, the inverted model, and the experimental data from ESAC. Calculated apparent phase velocities are derived using equation (6), proposed by Tokimatsu *et al.* (1992c).

Table 2  
Comparison of the *S*-Wave-Velocity Models from *PS* Logging and This Study

Layer No.	Thickness (m)	<i>PS</i> Logging Model (m/sec)	From ESAC Method (m/sec)
1	5.65	130.0	134.2
2	6.35	380.0	342.8
3	6.00	460.0	436.6
4	8.70	460.0	488.3
5	8.90	430.0	482.0
6	7.40	520.0	504.5
7	$\infty$		600.0

We conclude that the ESAC method gives more accurate results than the FK method in the detection of short-period Rayleigh wave dispersion that is composed not only of the fundamental mode but also of the higher mode. Note that this conclusion is obtained from the microtremor records of arbitrarily shaped array measurements, which were analyzed only by the FK method. It demonstrates that the ESAC method has the potential to estimate a shallow velocity structure that controls the seismic amplification in a high-frequency range. Although our array configuration is not ideal, we consider that similar situations will exist when microtremor-array measurements are carried out in urban areas. We believe that this study will inspire others to apply this technique, even in such conditions, to obtain accurate

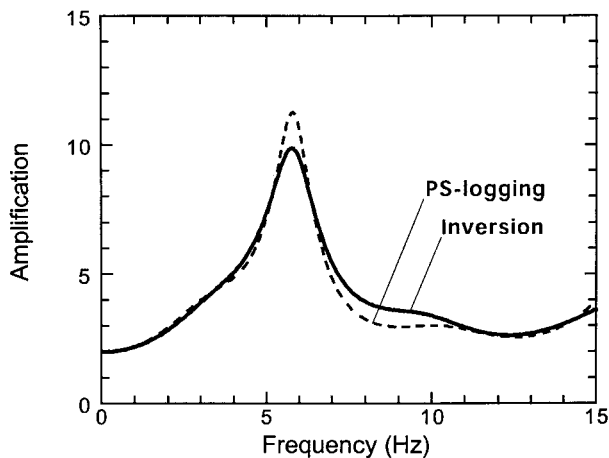


Figure 8. Comparison of the site-response amplification functions due to the  $SH$  wave vertical incidence for the  $PS$  logging model and estimated model from inversion of phase velocity results from the ESAC method.

phase-velocity dispersions and to explore underground structures to appropriately evaluate strong ground motion.

### Acknowledgments

We express sincere thanks to Prof. M. Horike, Osaka Institute of Technology, and Mr. T. Kagawa, Geo-Research Institute, Osaka, for their encouragement on this study. In calculating the Rayleigh wave dispersions, the FORTRAN code of "normal.f" by Prof. Y. Hisada, Kogakuin University, was used with slight modifications. A part of the work was carried out while one of us (M.O.) was at Stanford University as a visiting scholar on leave from Obayashi Corporation. We also thank Prof. A. S. Kiremidjian, Stanford University, for her encouragement of this study during M.O.'s stay. Constructive comments from Dr. William Walter, Associate Editor, and two anonymous reviewers were helpful in the improvement of the manuscript. We deeply appreciate the patient work of Dr. William Walter. Finally, one of us (M.O.) expresses his gratitude to Mr. Maurice Tarplee, Peninsula Engineering & Contracting Co., who was the first reader of the manuscript, who passed away 4 March, 1999.

### References

- Aki, K. (1957). Space and time spectra of stationary stochastic waves, with special reference to microtremors, *Bull. Earthquake Res. Inst.* **35**, 415–456.
- Aki, K. (1964). A note on the use of microseisms in determining the shallow structures of the earth's crust, *Geophysics* **29**, 665–666.
- Asten, M. W., and J. D. Henstridge (1984). Array estimators and the use of microseisms for reconnaissance of sedimentary basins, *Geophysics* **49**, 1828–1837.
- Capon, J. (1969). High-resolution frequency-wavenumber spectrum analysis, *Proc. IEEE* **57**, 1408–1418.
- Chouet, B., G. De Luca, G. Milina, P. Dawson, M. Martini, and R. Scarpa (1998). Shallow velocity structure of Stromboli Volcano, Italy, derived from small-aperture array measurements of Strombolian tremor, *Bull. Seism. Soc. Am.* **88**, 653–666.
- Harkrider, D. G. (1964). Surface waves in multilayered elastic media I. Rayleigh and Love waves from buried sources in a multilayered elastic half-space, *Bull. Seism. Soc. Am.* **54**, 627–680.

- Horike, M. (1985). Inversion of phase velocity of long-period microtremors to the  $S$ -wave-velocity structure down to the basement in urbanized areas, *J. Phys. Earth* **33**, 59–96.
- Horike, M. (1996). Geophysical exploration using microtremor measurements, in *10th World Conference on Earthquake Engineering*, Acapulco, Mexico, 23–26 June 1996, Paper No. 2033, Elsevier Science, Amsterdam, CD-ROM.
- Ishida, H., T. Nozawa, and M. Niwa (1998). Estimation of deep surface structure based on phase velocities and spectral ratios of long-period microtremors, in *The Effects of Surface Geology on Seismic Motion*, K. Irikura, K. Kudo, H. Okada, and T. Sasatani (Editors), A. A. Balkema, Rotterdam, 697–704.
- Kagawa, T. (1996). Estimation of velocity structures beneath Mexico City using microtremor array data, in *10th World Conference on Earthquake Engineering*, Acapulco, Mexico, Paper No. 1179, Elsevier Science, Amsterdam, CD-ROM.
- Kagawa, T., S. Sawada, Y. Iwasaki, and A. Nanjo (1998).  $S$ -wave velocity structure model of the Osaka sedimentary basin derived from microtremor array observations, *Jisin* **51**, 31–40 (in Japanese with English abstract).
- Kataoka, S., and H. Kawase (1998). Estimation of underground structure at Higashinada Ward, Kobe using surface wave of microtremor and explosion record, *Jisin* **51**, 99–112 (in Japanese with English abstract).
- Kawase, H. (1996). The cause of the damage belt in Kobe: the basin-edge effect, constructive interference of the direct  $S$ -wave with the basin-induced diffracted/Rayleigh waves, *Seism. Res. Lett.* **67**, no. 5, 25–34.
- Kawase, H., T. Satoh, T. Iwata, and K. Irikura (1998).  $SW$ -wave velocity structure in the San Fernando and Santa Monica areas, in *The Effects of Surface Geology on Seismic Motion*, K. Irikura, K. Kudo, H. Okada, and T. Sasatani (Editors), A. A. Balkema, Rotterdam, 733–740.
- Kudo, K., T. Kanno, H. Okada, O. Özel, M. Erdik, T. Sasatani, S. Higashi, M. Takahashi, and K. Yoshida (2002). Site-specific issues on strong ground motions during the Kocaeli, Turkey, earthquake of 17 August 1999, *Bull. Seism. Soc. Am.* **92**, 448–465.
- Lacoss, R. T., E. J. Kelly, and M. N. Toksoz (1969). Estimation of seismic noise structure using arrays, *Geophysics* **34**, 21–38.
- Ling, S., and H. Okada (1993). An extended use of the spatial autocorrelation method for the estimation of structure using microtremors, in *Proc. of the 89th SEGJ Conference*, Nagoya, Japan, 12–14 October 1993, Society of Exploration Geophysicists of Japan, 44–48 (in Japanese).
- Liu, H.-P., D. Boore, W. B. Joyner, D. H. Oppenheimer, R. E. Warrick, W. Zheng, J. C. Hamilton, and L. T. Brown (2000). Comparison of phase velocity from array measurements of Rayleigh waves associated with microtremor and results calculated from borehole shear-wave velocity profiles, *Bull. Seism. Soc. Am.* **90**, 666–678.
- Marquardt, D. W. (1963). An algorithm for least squares estimation of nonlinear parameters, *J. Soc. Indust. Appl. Math.* **11**, 431–441.
- Matsuoka, T., N. Umezawa, and H. Makishima (1996). Experimental studies on the applicability of the spatial autocorrelation method for estimation of geological structures using microtremors, *Butsuri-Tansa* **49**, 26–41 (in Japanese with English abstract).
- Matsushima, T., and H. Okada (1989). A few remarks on the scheme of observation and analysis in estimating deep geological structures by using long-period microtremors, *Geophys. Bull. Hokkaido Univ.* **52**, 1–10 (in Japanese with English abstract).
- Matsushima, T., and H. Okada (1990). Determination of deep geological structures under urban areas using long-period microtremors, *Butsuri-Tansa* **43**, 21–33.
- Milana, G., S. Barba, E. Del Pezzo, and E. Zambonelli (1996). Site response from ambient noise measurements: new perspective from an array study in Central Italy, *Bull. Seism. Soc. Am.* **86**, 320–328.
- Miyakoshi K., H. Okada, T. Sasatani, T. Moriya, S. Ling, and S. Saito (1994). Estimation of geological structure under ESG blind prediction

- test sites in Odawara city by using microtremors, (*J. Seism. Soc. Jpn.*) **47**, 273–285 (in Japanese with English abstract).
- Miyakoshi, K., and H. Okada. (1996). Estimation of the site response in the Kushiro City, Hokkaido, Japan, using microtremors with seismometer arrays, in *10th World Conference on Earthquake Engineering*, Acapulco, Mexico, Paper No. 900, Elsevier Science, Amsterdam, CD-ROM.
- Miyakoshi, K., T. Kagawa, and S. Kinoshita (1998). Estimation of geological structures under Kobe area using the array recordings of microtremors, in *The Effects of Surface Geology on Seismic Motion*, K. Irikura, K. Kudo, H. Okada, and T. Sasatani, (Editors). A. A. Balkema, Rotterdam, 691–696.
- Nelder, J. A., and R. Mead (1965). A simplex method for function minimization, *Comp. J.*, **7**, 308–313.
- Okada, H. (1986). A research on long period microtremor array observations and their time and spatial characteristics as probabilistic process, report of a Grant-in-Aid for Co-operative Research (A) No. 59340026 supported by the Scientific Research Fund in 1985 (in Japanese).
- Okada, H., K. Matsushima, and E. Hidaka (1987). Comparison of spatial autocorrelation method and frequency-wavenumber spectral method of estimating the phase velocity of Rayleigh waves in long-period microtremors, *Geophys. Bull. Hokkaido Univ.* **49**, 53–62 (in Japanese with English abstract).
- Okada, H. (1994). A research on the practical application of microtremor exploration technique to a wide area survey of a underground structure under 3,000 m in depth, report of a Grant-in-Aid for Co-operative Research (B) No. 03554009 supported by the Scientific Research Fund in 1993 (in Japanese).
- Sato, T., H. Kawase, M. Matsui, and S. Kataoka (1991). Array measurement of high frequency microtremors for underground structure estimation, in *Proc. of the 4th International Conference on Seismic Zonation*, Stanford, California, 25–29 August 1991, Earthquake Engineering Research Institute, Vol. 2, 409–416.
- Satoh, T., H. Kawase, and S. Matsushima (2001). Estimation of S-wave velocity structures in and around the Sendai Basin, Japan, using array records of microtremors, *Bull. Seism. Soc. Am.* **91**, 206–218.
- Shima, E., M. Yanagisawa, K. Kudo, T. Yoshii, K. Seo, and K. Kuroha (1978). On the base rock of Tokyo, part 3: observations of seismic waves generated from the 4th and 5th Yumenoshima explosions, *Bull. Earthquake Res. Inst.* **53**, 305–318 (in Japanese with English abstract).
- Suetomi, I., and S. Nakamura. (1996). Spectral characteristics and nonlinear effects during recent large earthquakes observed at Kushiro City, Japan, in *10th World Conference on Earthquake Engineering*, Acapulco, Mexico, Paper No. 1476, Elsevier Science, Amsterdam, CD-ROM.
- Tokimatsu, K., K. Shinzawa, S. Kuwayama, and A. Abe (1991). Estimation of Vs profiles from Rayleigh wave dispersion data at site affected in the Loma Prieta Earthquake, in *Proc. of the 4th International Conference on Seismic Zonation*, Stanford, California, 25–29 August 1991, Earthquake Engineering Research Institute, Vol. 2, 507–514.
- Tokimatsu, K., Y. Miyadera, and S. Kuwayama (1992a). Determination of shear wave velocity structures from spectrum analyses of short-period microtremors, in *Proc. 10th World Conference on Earthquake Engineering*, Madrid, Spain, 19–24 July 1992, A. A. Balkema, Rotterdam, Vol. 1, 253–258.
- Tokimatsu, K., K. Shinzawa, and S. Kuwayama (1992b). Use of short-period microtremors for Vs profiling, *J. Geotech. Eng. ASCE* **118**, 1544–1558.
- Tokimatsu, K., S. Tamura, and H. Kojima (1992c). Effects of multiple modes on Rayleigh wave dispersion characteristics, *J. Geotech. Eng. ASCE* **118**, 1529–1543.
- Yamanaka, H., M. Takemura, H. Ishida, T. Ikeura, T. Nozawa, T. Sasaki, and M. Niwa (1994). Array measurements of long-period microtremors and estimation of S-wave velocity structure in the western part of the Tokyo metropolitan area, (*J. Seism. Soc. Jpn.*) **47**, 163–172 (in Japanese with English abstract).

Technical Research Institute  
Obayashi Corporation  
4-640 Shimo-Kiyoto, Kiyose  
Tokyo 204-0011, Japan

Manuscript received 11 July 1998.